

# Miniemulsion Living Free Radical Polymerization by RAFT

Alessandro Butté, Giuseppe Storti, and Massimo Morbidelli\*

ETH Zürich, Laboratorium für Technische Chemie (LTC), CAB, Universitätstr. 6,  
CH-8092 Zürich, Switzerland

Received December 15, 2000; Revised Manuscript Received April 23, 2001

**ABSTRACT:** Various living mechanisms have been used in bulk polymerization to produce via free radical polymerization both controlled polymers, i.e., with low polydispersity, and block copolymers. The common drawback of all these processes is the very low polymerization rate which derives from the decreased concentration of propagating radicals. This problem can be overcome in principle by operating in emulsion polymerization, so as to take advantage of radical segregation to decrease terminations without significantly reducing the polymerization rate with respect to the corresponding nonliving processes. In this work, it has been shown that this result can be achieved only using the RAFT (or degenerative transfer) living mechanism and operating in miniemulsion polymerization. Several experiments are presented where, using different monomers, living conditions are achieved without significant loss in productivity. The obtained results are supported by modeling arguments, which also rationalize previous experimental results reported in the literature using different living mechanisms.

## 1. Introduction

Free radical polymerization (FRP) is widely used in industrial practice, in both homogeneous (bulk and solution) and heterogeneous (emulsion and suspension) processes, largely due to its mild reaction conditions.<sup>1,2</sup> FRP can in fact easily operate in the presence of impurities, such as residuals of inhibitor and oxygen traces, and in a large temperature range. Moreover, the development of the so-called living radical polymerization (LRP; cf. Matyjaszewski<sup>3</sup>) at the beginning of the 1990s represents a chance to further broaden the application spectrum of this process. By LRP it is in fact possible to overcome two major drawbacks of FRP: the lack of control of the polymer molecular weight and the inability to produce block copolymers.

Different approaches have been proposed to carry out LRP. Among them, it is worth mentioning nitroxide-mediated polymerization<sup>4</sup> (NLP), atom transfer living polymerization<sup>5</sup> (ATRP), degenerative transfer<sup>6</sup> (DT), and reversible addition–fragmentation transfer<sup>7</sup> (RAFT) polymerization. Despite the differences among the reaction mechanisms involved in these processes, the underlying concept is the same: since it is impossible to have all the polymer chains growing throughout the entire process because of the presence of fast bimolecular terminations, most of the chains are reversibly trapped by a so-called “trapping agent”, a molecular species the nature of which identifies the particular living mechanism. These trapped chains, usually called “dormant” chains, are unable to propagate but also to terminate. Therefore, the probability of termination is largely reduced with respect to that of chain growth, since bimolecular termination is second order with respect to radical concentration, while propagation is only first order. Accordingly, the relevance of termination events can strongly decrease, thus leading to a negligible amount of terminated chains with respect to the overall amount of chains (including dormant and dead chains) at the end of the process. However, since terminations are anyhow present, this polymerization is also referred to as pseudo-living radical polymerization, to highlight the difference with respect to an intrinsically living polymerization such as ionic polym-

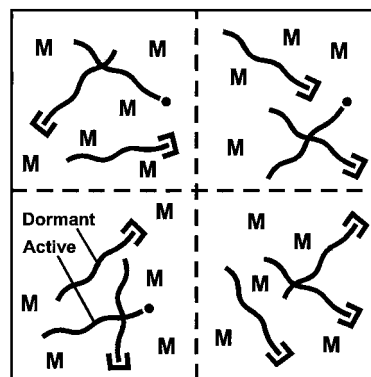


**Figure 1.** Segregation of the polymerization medium, represented by the presence of the dashed lines, reduces radical bimolecular terminations.

erization. The second essential element of living polymerization is that the reversible trapping mechanism forces each growing chain to undergo a series of active and dormant time periods. If the exchange between the two states is fast enough, so that every chain experiences many active periods during its lifetime, the typical continuous growth of true living mechanisms is approached, thus resulting in rather homogeneous final distributions of chains. For example, the MWD of a homopolymer produced by LRP is narrower than that obtained in the corresponding nonliving polymerization.

When dealing with LRP in homogeneous systems (e.g., bulk or solution polymerization), the only way to approach living conditions is to reduce radical concentration. Of course, this is a major drawback, since the polymerization rate and, therefore, productivity are also reduced, thus decreasing the potential of the process for industrial applications. On the other hand, it is well-known that chain segregation, which is present in heterogeneous processes such as emulsions, prevents termination while preserving the overall concentration of active chains. This is schematically shown in Figure 1, where the role of active chain segregation into smaller and smaller reaction loci is shown to reduce the probability of radical collision. While without segregation each radical can terminate with all the others, when

segregated to such an extent that each radical is "isolated" in a single reaction locus, terminations are no longer possible. This ideal situation can be approached in emulsion polymerization in the so-called "zero-one" limit,<sup>2</sup> where a radical present alone in a particle can terminate only with a new radical entering the particle, which is the case when the rate of bimolecular termination becomes controlled by radical entry. This corresponds to the fact that as soon as a radical enters a particle containing already one radical, the two terminate instantaneously, thus leading to the characteristic "zero-one" system. This leads to larger polymerization rates and larger molecular weights than in the corresponding bulk processes.

The aim of this work is to take advantage of the "intrinsic" reduction of bimolecular terminations typical of segregated systems to carry out a LRP at a reaction rate larger than that of the corresponding bulk processes and actually comparable to that of the corresponding nonliving processes. The paper is organized as follows: First, previous experimental results reported in the literature are reviewed. Then, different operating modes to carry out an emulsion LRP are discussed, and based on considerations about the kinetic behavior of the system, the most convenient operating conditions to couple radical segregation and living polymerization are identified. Finally, a few experiments using different monomers are reported in order to demonstrate the reliability of the proposed process.

## 2. Previous Work

In this section, previous literature results on LRP in emulsion are analyzed, by separately considering the different adopted living mechanisms, i.e., NLP, ATRP, DT, and RAFT.

The first LRP carried out in a heterogeneous system was reported by Bon et al.<sup>8</sup> It was shown that living polymers by NLP of styrene with TEMPO at 135 °C can be obtained using a seeded emulsion polymerization. In particular, polystyrene with a final polydispersity value around 1.5 was produced, with practically complete conversion in 36 h. Satisfactory results have been also obtained by Marestin et al.<sup>9</sup> using an *ab initio* emulsion polymerization. They showed that, after an optimal choice of the nitroxide, polymerization rates similar to those reported by Bon et al.<sup>8</sup> can be obtained without a significant amount of flocculation.

A different approach was used by Prodpran et al.<sup>10</sup> and MacLeod et al.,<sup>11</sup> who used miniemulsion polymerization, thus avoiding all problems connected to particle nucleation. The obtained latex was shown to be stable even at the high temperature characteristic of NLP (120–135 °C). A typical living behavior was observed, with linearly increasing average molecular weight ( $M_n$ ) and low polydispersity ( $P_d$ ) values (1.1–1.7). However, the polymerization time, as shown by Prodpran et al.,<sup>10</sup> was comparable to or even larger than that of the corresponding bulk polymerization. This result was recently confirmed by Farcet et al.,<sup>12</sup> who performed a miniemulsion polymerization using a nitroxide able to work at 90 °C.

LRP in emulsion<sup>13–15</sup> and miniemulsion<sup>16</sup> of different monomers was also reported by Matyjaszewski and co-workers, using ATRP as living mechanism. It was shown that, by a suitable choice of surfactant (nonionic) and initiator, it is possible to obtain stable latexes exhibiting a living behavior, as indicated by the almost

linear growth of  $M_n$  with conversion and the low  $P_d$  values. However, also in this case a direct comparison of the kinetics for bulk and emulsion polymerizations of *n*-butyl methacrylate shows that the obtained rates are very similar. The same conclusion applies to all the other considered monomers, i.e., methyl methacrylate, styrene, and butyl acrylate, although a direct comparison was not reported.

The use of DT in miniemulsion LRP was shown to be very effective in producing stable latexes exhibiting a large enhancement of the polymerization rate with respect to the corresponding bulk polymerization. Both Lansalot et al.<sup>17</sup> and Butté et al.<sup>18</sup> reported that after about 2 h almost complete conversion was obtained when polymerizing styrene at temperatures ranging from 70 to 80 °C using  $C_6F_{13}I$  as transfer agent. Similar results were obtained using both water-soluble (4,4'-azobis(4-cyanopentanoic acid)) and oil-soluble ( $\alpha,\alpha'$ -azobis(butyronitrile)) initiators. These polymerization rates are very close to those typical of nonliving emulsion polymerization with styrene and considerably larger than those of the corresponding living bulk process. In all cases,  $M_n$  exhibited a linear behavior, and the polydispersity value ranged from 1.5 to 1.9. It is worth noting that Lansalot et al.<sup>17</sup> reported that the same reaction carried out in *ab initio* emulsion resulted in a very poor control of the polymer growth:  $M_n$  was larger than the theoretical one (given by the molar ratio between initial concentrations of monomer and transfer agent), with  $P_d$  values from 1.8 to 2. The authors explained this result as due to the very poor efficiency of the transfer agent which, due to its high hydrophobicity, diffuses very slowly (and probably not completely) from the monomer droplets to the polymer particles. Farcet et al.<sup>19</sup> also reported the application of DT in miniemulsion to the production of styrene–butyl acrylate block copolymers.

The use of the RAFT living mechanism in *ab initio* emulsion polymerization was reported by several groups.<sup>20–22</sup> Rather different results have been presented, although some common points can be identified. In the work by Uzulina et al.,<sup>20</sup> problems of poor latex stability and slow diffusion of the chain transfer agent through the water phase were reported. Good results (a linear increase of  $M_n$  with conversion and small  $P_d$  values, between 1.5 and 2) were obtained only when using a water-soluble transfer agent. On the other hand, when using a scarcely water-soluble chain transfer agent, living conditions could be approached only with large amounts of initiator and with relatively large  $P_d$  values. No data of polymerization rate were reported, with the exception of the case of methyl methacrylate, where a very large polymerization time (18% conversion in 1 h) was reported. In the works by Charmot et al.<sup>21</sup> and by Moad et al.,<sup>22</sup> no problems of latex stability were observed. The transfer agent was charged to the reactor at the beginning with only a small portion of the monomer, while the rest was fed during polymerization. The experimental results indicated that the transfer agent was completely consumed in the early stage of the polymerization<sup>21</sup> and that the average molecular weight was growing linearly with conversion, thus confirming the living nature of the polymerization. While Charmot et al.<sup>21</sup> reported rather large polydispersity values (from 2.1 to 3.3 in the case of styrene and from 1.4 to 2.3 in the case of butyl acrylate), Moad et al.<sup>22</sup> reported that the final polydispersity was strongly

affected by the nature of the transfer agent ( $P_d$  values ranging from 1.37 to 7.09). More recently, a work about a copolymerization of styrene and butyl acrylate appeared in the literature<sup>23</sup> showing how this technique may have important applications, e.g., in the film formation.

Finally, Monteiro and co-workers have reported the application of RAFT under seeded<sup>24</sup> and miniemulsion<sup>25</sup> conditions. They demonstrated the possibility of producing several different styrene and methacrylate homopolymers with low polydispersities and large polymerization rates. In addition, it was shown that these techniques may also be applied to block copolymers to achieve higher block purities than in solution processes due to the reduced amount of bimolecular terminations. It was also shown that the desorption of the leaving group of the RAFT agent can influence the final polymerization rate. We will come back to comment on this later on in this work.

### 3. Choice of the Living Mechanism

The literature results reviewed above can be rationalized through appropriate arguments about the kinetics of the involved phenomena, leading to an insight in the system behavior which can indicate how to best couple living polymerization with radical segregation. Let us first consider NLP and ATRP: good results are reported in the literature,<sup>10–16</sup> in particular when using miniemulsion polymerization. However, small polymerization rates, comparable to those of the corresponding bulk process, have always been reported. These findings could be ascribed to the particular activation–deactivation mechanism characterizing the living process when using NLP and ATRP, which is given by



where  $R_n^\bullet$  represents an active chain with  $n$  monomer units,  $D_n$  a dormant chain with  $n$  monomer units,  $k_a$  and  $k_d$  the reaction rate constants of activation and deactivation, respectively, and  $X$  and  $Y$  two molecular species with different meaning depending on the specific living mechanism under consideration. In particular, when dealing with NLP using TEMPO,  $X$  represents the TEMPO radical and  $Y$  is not present, since the reaction is a simple reversible termination between two radicals (i.e., the polymer and the nitroxide radical). On the other hand, in the case of ATRP, where the living mechanism is given by a redox reaction,  $X$  represents the metal in the oxidized form and  $Y$  in the reduced form.

As mentioned above, to have a good homogenization of the polymer chains, the dormant chains should add only a few units during each activation period. This means that in general the activation–deactivation reactions must have frequencies comparable to propagation. Therefore, due to the specific stoichiometry of the activation–deactivation mechanism of NLP and ATRP, these reactions are also dominating in the determination of the number of active radicals per particle. Radical entry is in fact much less probable, and bimolecular termination occurs only when two consecutive activation events take place. Consequently, the particle moves continuously from a situation without radicals to one with 1 radical (referred to in the following as state 0 and state 1, respectively), and the expected time evolution of the number of active chains per particle exhibits

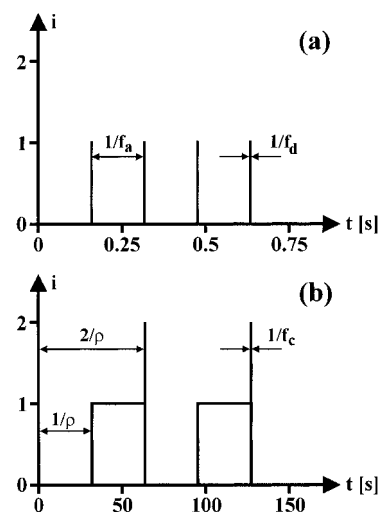


**Figure 2.** Schematic representation of the time evolution of the number of active chains per particle,  $i$ , for (a) emulsion with NLP or ATRP and (b) emulsion with DT or RAFT.

the qualitative behavior shown in Figure 2a. It is worth noting that the time a particle spends in state 0 and 1 is determined by the frequencies of activation ( $f_a$ ) and deactivation ( $f_d$ ). To express these frequencies for a particle of volume  $V_p$  with a molar concentration  $D$  of dormant chains, let us consider NLP with TEMPO. The following relations apply:

$$f_a = k_a D N_A V_p \quad (2)$$

$$f_d = \frac{k_d n_{\text{TEMPO}}}{N_A V_p} \quad (3)$$

where  $n_{\text{TEMPO}}$  represents the number of molecules of TEMPO in the particle and  $N_A$  is Avogadro's constant. It is clear from Figure 2a that the average number of active chains per particle can be estimated as the fraction of time spent by the particle in state 1, i.e.,  $(1/f_d)/(1/f_a + 1/f_d)$ . If typical values for  $k_a$ ,  $k_d$ , and  $D$  are considered as taken from the literature<sup>26</sup> ( $k_a = 0.001$  1/s,  $k_d = 5 \times 10^7$  L/(mol s),  $D = 0.025$  mol/L) and considering a 100 nm particle with one single molecule of TEMPO ( $n_{\text{TEMPO}} = 1$ ), the average number of radicals per particle is estimated as 0.05. This is 1 order of magnitude smaller than 0.5, the characteristic value of the corresponding nonliving emulsion polymerization, and justifies the observed slow polymerization rates.<sup>10–14</sup>

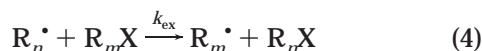
One could argue that this situation could be improved by increasing the activation frequency,  $f_a$ , and making it closer to the deactivation one,  $f_d$ . This, by the way, should also enhance the number of activation periods, thus producing a more homogeneous growth of the polymer chains. However, from Figure 2a, it is clear that the more the frequency of activation approaches that of deactivation, the more the occurrence of a second activation becomes probable when the first activated radical is still present in the particle. At this point, a bimolecular termination of the two radicals is immediate because of the very small particle size, resulting in the formation of a dead chain and in the accumulation of two TEMPO radicals inside the particle. As a consequence, the frequency of deactivation is increased, thus moving back the system to small  $f_a/f_d$  ratios.

Thus, summarizing, because the living mechanisms affect the number of radicals per particle, NLP and



ATRP always lead to small polymerization rates. This is so because the number of radicals per particle is always extremely small, since the frequency of activation is much smaller than that of deactivation. If this is not the case, not only too many dead chains are generated, but also the trapping agent molecules accumulate inside the particle, thus self-increasing the deactivation frequency and, therefore, going back to the situation of deactivation faster than activation. It is worth noting that this mechanism closely resembles the persistent radical effect present in homogeneous systems,<sup>27</sup> where the trapping agent concentration self-adjusts itself in order to decrease terminations, as also discussed recently by Charleux.<sup>28</sup>

On the other hand, experiments with DT and RAFT as living mechanisms indicate that a considerable increase of the polymerization rate (compared to the corresponding bulk processes) can be obtained.<sup>17–24</sup> This result can be explained by considering the stoichiometry of the transfer (or exchange) reaction which constitutes the living mechanism of DT or RAFT, where, as opposed to NLP and RAFT, the living reaction does not affect the concentration of the active chains:



where dormant chains are indicated by  $R_n X$  to evidence the role of the transfer agent  $X$ . In this case, in a particle containing one active chain and several dormant chains, the radical can transfer its activity to different dormant chains until a second radical enters the particle. At this time, a very fast bimolecular termination takes place. In other words, the number of radicals per particle in this case is controlled only by radical entry, since the faster exchange reactions are not relevant. This is sketched in Figure 2b, where the time evolution of the number of active chains per particle is shown as determined by the frequency of radical entry ( $\rho$ ) and bimolecular termination ( $k_t$ ). It is clear that this is the same situation of a classical (i.e., nonliving) emulsion polymerization, and therefore the two processes exhibit similar polymerization rates. In addition, it is worth noting that in this frame since termination occurs every two successive radical entries in the same particle, the number of dead chains can be controlled by properly controlling the frequency of radical entry. In the case of the “zero-one” system,<sup>2</sup> this does not affect the average number of radicals per particle, so that living conditions can be achieved without affecting the polymerization rate.

This analysis allows us to conclude that the only way to take advantage of the radical segregation effect typical of emulsion polymerization in order to increase the rate of LRP is to use RAFT or DT as living mechanisms. The results of a deeper theoretical analysis on the differences between the use of NLP, ATRP, RAFT, and DT are reported elsewhere,<sup>29</sup> leading to identical conclusions. We should note in this context that while DT with iodine can be applied with good results only to styrene (its use with butyl acrylate or methyl methacrylate seems to be problematic<sup>30</sup>), RAFT has been proved more flexible and can be applied to a broader range of monomer types.<sup>22</sup>

The next problem is to realize in practice a RAFT or DT polymerization in emulsion. With this respect, the chemical species carrying the transfer agent,  $X$  (cf. eq 4), indicated in the following as RAFT agent, has to

satisfy two basic requirements. First, the RAFT agent has to be in the reaction loci (particles) since the beginning of the polymerization, so that all chains experience the same lifetime. Second, the transfer agent has to be homogeneously distributed among the particles, so that the same average molecular weight can be obtained in all particles.

Let us first see how these two requirements can be fulfilled using an *ab initio* emulsion polymerization. At the beginning we have droplets containing monomer and RAFT agent, from which both species have to diffuse to the polymer particles, as soon as these are nucleated. In this frame, it is clear that the first requirement above can be satisfied only if the RAFT agent is sufficiently water-soluble so as to diffuse in the polymer particles in a time short enough compared to the duration of the polymerization. A problem of this type has been described by Lansalot et al.,<sup>17</sup> who reported that the living agent ( $C_6F_{13}I$ ) was not completely consumed even at the end of the polymerization due to its poor compatibility with water. This indicated that the RAFT agent entered the reaction loci continuously during the entire process. Since each of such entry corresponds to the start of a new radical chain, this caused a broadening of the MWD and, thus, large polydispersity values.

About the second requirement, i.e., the need of distributing the RAFT agent homogeneously among all the particles, we must consider the duration of the process of particle generation, i.e., nucleation. In particular, we require that the nucleation period should be much faster than the period of diffusion of the RAFT agent from the monomer droplets. If this is not the case, then the particles that nucleated first received the RAFT agent from the droplets for a longer time than those nucleated later. This leads to different concentrations of dormant species in the particles, and then to a broadening of the MWD, resulting from the superposition of narrow “local” distributions with different average values. This is probably the reason that in some experimental studies<sup>22,23</sup> larger polydispersity values have been obtained in emulsion than in bulk, using otherwise similar conditions. Combining the two requirements above, we can conclude that in order to use *ab initio* emulsion polymerization for LRP, one has to carefully tune the durations of the RAFT agent diffusion and the nucleation processes, to have the second much faster than the first one, which in turn should be much faster than the polymerization process. This is not easy to realize in practice, and it could explain the otherwise unexpected difficulties which are often found in practice when dealing with *ab initio* emulsion LRP. A confirmation of the arguments presented above is found in the Appendix, where a suitable simplified mathematical model has been developed to describe the diffusion of the RAFT agent to the polymer particles.

On the other hand, alternative operating modes exist where this difficulty can be overcome. This is the case of the polymerization carried out in miniemulsion or starting from a preformed seed. In both cases, the dormant species can be directly and uniformly introduced in the polymerization loci before starting the reaction, thus satisfying both the above requirements.

In the following, some applications of miniemulsion polymerization to the synthesis of homo- and copolymers by RAFT are discussed in order to demonstrate the reliability of the process. It is worth noting that mini-

**Table 1. Operating Conditions and Results of the Experimental Runs Carried Out in Presence of Various Monomers and RAFT Agents (Cf. Table 2)<sup>a</sup>**

run	monomer	RAFT agent	$M_0/D_0$	$M_0/I_0$	$T(^{\circ}\text{C})$	$\chi$	$t$ (min)	$M_n$ (g/mol)	$P_d$
1	STY	<b>1</b>	490.5	2043	80	67.0	116	37 860	1.36
2	STY	<b>2</b>	654.8	2213	80	10.8	60	7 030	1.30
3	STY	<b>2</b>	576.0	1209	80	39.4	132	19 100	1.43
4	STY	<b>3</b>	800.2	1040	75	90.1	61	142 820	3.58
5	STY	<b>4</b>	370.4	1975	80	89.4	112	35 140	2.00
6	STY	<b>4</b>	500.9	2555	75	83.5	134	43 690	1.75
7	MMA	<b>5</b>	435.3	2015	65	90.2	15	46 510	2.01
8	STY	<b>PMMA 7</b>	380.3	0	75	93.1	20	81 450	2.44
9	MMA	<b>6</b>	500.0	200	65	91.0	8	47 460	1.94
10	STY	<b>PMMA 9</b>	416.8	639	70	87.7	26	102 540	2.97
11	STY	<b>3</b>	197.3	800	70	62.6	174	12 260	1.38
12	BA	<b>PSTY 11</b>	122.6	0	70	98.0		29 110	1.92

<sup>a</sup> Reactions have been carried using 30 g of monomer, 170 g of water, 1 g of hexadecane, and 0.5 g of sodium dodecyl sulfate. Symbols:  $M_0$ ,  $D_0$ , and  $I_0$ , initial concentrations of monomer, RAFT agent, and initiator (potassium persulfate), respectively;  $T$ , temperature;  $\chi$ , conversion;  $t$ , reaction time;  $M_n$  and  $P_d$ , number-average molecular weight and polydispersity.

emulsion polymerization has been preferred to seeded polymerization since the latter introduces a limited amount of polymer grown under nonliving conditions (i.e., the seed), which may not be acceptable when producing highly homogeneous products.

#### 4. Experimental Part

**Materials.** All chemicals were used as received: styrene (monomer, STY,  $\geq 99\%$ , Aldrich), methyl methacrylate (monomer, MMA,  $\geq 99\%$ , Fluka), butyl acrylate (monomer, BuA,  $\geq 99\%$ , Fluka), potassium peroxodisulfate (radical initiator, KPS,  $\geq 99\%$ , Fluka), sodium dodecyl sulfate (surfactant, SDS,  $\geq 99\%$ , Fluka), sodium hydrogen carbonate (chemical buffer,  $\text{NaHCO}_3$ ,  $\geq 99.5\%$ , Fluka), hexadecane (stabilizer, HD,  $\geq 98\%$ , Fluka). Water was always doubly distilled before use.

**Miniemulsion Reaction.** All reactions, whose recipes are given in the next section, were carried out according to the following procedure. The miniemulsion was prepared by mixing the oil phase (monomer, polymer, stabilizer, and transfer agent) with the water phase (water and surfactant) under vigorous mechanical agitation for 10 min. This step was followed by further mixing under agitation in an ultrasonic homogenizer equipped with a cylindrical probe (B.Braun Labsonic 1510) at a power of 30 W for 20 min. The resulting mixture, which already looked like emulsion, was passed 10 times in a microfluidizer (Microfluidics, model 110-Y, chamber F20Y) at an inlet pressure of 200 bar. The final miniemulsion was long enough stable with respect to the reaction time. This mixture was then charged to a cylindrical reactor, equipped with magnetic stirrer, water condenser, and baffles. Before the reaction started, the reactor was purged with nitrogen for 30 min. The temperature was controlled within  $\pm 1^{\circ}\text{C}$  by a jacket connected to a thermostatic bath circulating a silicon oil. Initiator and  $\text{NaHCO}_3$  were diluted in 4 mL of water and added to the system when the reaction temperature was reached. From that time the reaction started and samples were withdrawn at regular time intervals with a syringe.

**Samples Characterization.** Conversion was measured gravimetrically and particle diameter by dynamic light scattering (Malvern ZetaSizer 5000). MWD measurements were carried out by gel permeation chromatography (GPC) in a Hewlett-Packard apparatus (series 1100) equipped with three columns (Polymer Standards, Plgel 5 $\mu$ , Mixed-C). The apparatus was calibrated by polystyrene standards (Polymer Standards), and tetrahydrofuran was used as eluent (1 mL/min,  $40^{\circ}\text{C}$ ). The MWD was estimated by a GPC software provided by PSS (Polymer Standard Service, Mainz, Germany).

**Synthesis of the RAFT Agent 2.** A solution of (thiobenzoil)thioglycolic acid (0.01 mol, 99%, Aldrich) in 0.1 N NaOH (40 mL) was mixed with *tert*-butyl mercaptan (0.015 mol,  $\geq 98\%$ , Fluka). A dark violet oil separated immediately, and after 3 h, the oil was extracted with hexane, washed two times with 0.1 N NaOH, and dried over  $\text{MgSO}_4$ . After the removal of the solvent, the product is left under vacuum, giving an

almost complete yield.  $^1\text{H}$  NMR (acetone, 300 MHz): 7.82–7.88 (m, 2H, phenyl), 7.40–7.46 (m, 1H, phenyl), 7.26–7.35 (m, 2H, phenyl), 1.66 (s, 9H,  $\text{CH}_3$ ).  $^{13}\text{C}$  NMR (acetone, 50 MHz): 230.10, 131.59, 128.00, 126.54, 52.06, 28.16.

**Synthesis of the RAFT Agent 4.** This synthesis was carried out in three subsequent steps, as described in the following. Pyrrole (0.149 mol,  $\geq 97\%$ , Fluka), potassium hydroxide (0.164 mol, Siegfried CMS), and carbon disulfide (0.298 mol,  $\geq 99.9\%$ , Fluka) were mixed and left under agitation for 48 h at room temperature with air. The carbon disulfide in excess was extracted by vacuum from the solution, which appeared red-brown. The remaining solid was dissolved with ether, filtered, and dried, thus obtaining a brown powder, which was crystallized by acetone. About 10 g of product (potassium pyrrole-1-carbodithioate,  $\text{C}_4\text{H}_4\text{NCSSK}$ ) were recovered as a dark-yellow hygroscopic crystal.  $^1\text{H}$  NMR (acetone, 300 MHz): 8.20–8.18 (m, 2H, pyrrole), 6.01–5.99 (m, 2H, pyrrole).  $^{13}\text{C}$  NMR (acetone, 50 MHz): 219.49, 120.24, 108.80.

1-Phenylethanol (0.198 mol,  $\sim 96\%$ , Fluka) was diluted in 100 mL of ether and cooled to about  $0^{\circ}\text{C}$  with ice. 20 mL of phosphorus tribromide (0.212 mol,  $\geq 98\%$ , Fluka) diluted in 80 mL of ether was very slowly dropped into the solution and left for 20 h at room temperature under agitation. After cooling the solution to about  $0^{\circ}\text{C}$ , distilled water was added until no more gas formation was observed. The product was extracted with ether, washed with  $\text{H}_2\text{O}$ , and dried over  $\text{MgSO}_4$ . A liquid (33.47 g, 1-phenylethyl bromide,  $\text{CH}_2\text{BrCH}_2\text{C}_6\text{H}_5$ ) was obtained after evaporation of the solvent.  $^1\text{H}$  NMR (acetone, 300 MHz): 7.52–7.48 (m, 2H, phenyl), 7.39–7.27 (m, 3H, phenyl), 5.38 (q, 1H CH,  $J = 6.9$  Hz), 2.02 (d, 3H  $\text{CH}_3$ ,  $J = 6.9$  Hz).  $^{13}\text{C}$  NMR (acetone, 50 MHz): 143.57, 128.63, 128.30, 126.89, 49.92, 7.47.

Potassium *N*-pyrrole dithiocarbonate (0.0196 mol) was diluted in 10 mL of methanol and 1-phenylethyl bromide (0.0229 mol) dropped into the solution. The solution was left under reflux and agitation for about 16 h, and during the reaction, a white precipitate (KBr) was formed. Water was added, and the product was extracted by ether, washed with  $\text{H}_2\text{O}$ , and dried over  $\text{MgSO}_4$ . The final product was obtained as a dark red oil (2.99 g, pyrrole-1-carbodithioic acid 1-phenylethyl ester,  $\text{C}_4\text{H}_4\text{NCSSCH}_2\text{C}_6\text{H}_5$ ) after evaporation of the solvent and was further purified by chromatography (silica gel, hexane).  $^1\text{H}$  NMR (acetone, 300 MHz): 7.75–7.73 (m, 2H, pyrrole), 7.52–7.48 (m, 2H, phenyl), 7.41–7.27 (m, 3H, phenyl), 6.39–6.37 (m, 2H, pyrrole), 1.83 (d, 3H  $\text{CH}_3$ ,  $J = 7.1$  Hz), 1.49 (q, 1H CH,  $J = 7.1$  Hz).  $^{13}\text{C}$  NMR (acetone, 50 MHz): 199.00, 140.93, 128.71, 127.88, 120.52, 114.36, 50.76, 20.73.

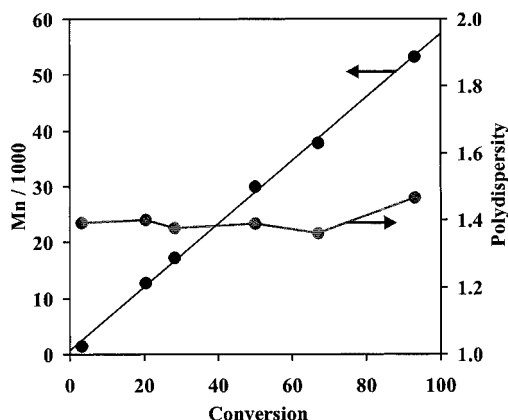
#### 5. Experimental Results

In the following, several experimental runs are discussed to illustrate the main features of RAFT polymerization in miniemulsion. All polymerization recipes and results are summarized in Table 1, while the RAFT agents used have the following general structure Z–CS–S–R, where the meaning of Z and R is reported in Table

**Table 2.** Chemical Structure (Z-CS-S-R) of the RAFT Agents Used in the Experimental Runs Reported in Table 1<sup>a</sup>

RAFT agent	Z	R	$M_n$	$P_d$
1	phenyl	-(STY) <sub>n</sub> C(CH <sub>3</sub> ) <sub>3</sub>	1470	1.39
2	phenyl	-C(CH <sub>3</sub> ) <sub>3</sub>		
3	pyrrole	-(STY) <sub>n</sub>	7380	1.12
4	pyrrole	-STY		
5	pyrrole	-(MMA) <sub>n</sub> C(CH <sub>3</sub> ) <sub>2</sub> CN	10340	1.34
6	pyrrole	-(MMA) <sub>n</sub> C(CH <sub>3</sub> ) <sub>2</sub> CN	7700	1.38

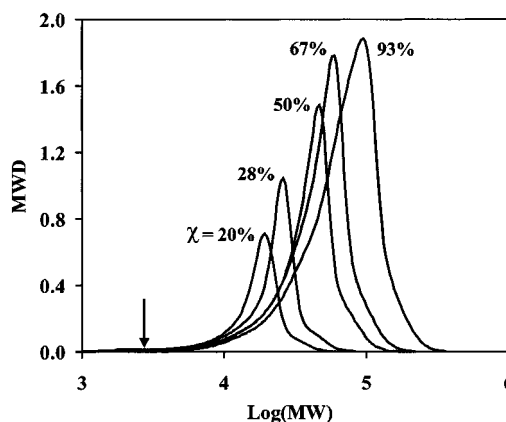
<sup>a</sup> Oligomeric RAFT agents (no. 1, 3, 5, 6) have been prepared by bulk polymerization at 100 °C in the case of styrene, in solution polymerization (50% toluene) at 70 °C initiated by AIBN in the case of methyl methacrylate.

**Figure 3.** Experimental values of the number-average molecular weight,  $M_n$  (g/mol), and the polydispersity as a function of conversion for a styrene miniemulsion LRP with RAFT agent 1 (run 1 in Table 1).

2. Note that RAFT agent 4 has been already used for bulk polymerization of MMA.<sup>31</sup>

In Figure 3, number-average molecular weight,  $M_n$ , and polydispersity,  $P_d$ , for a styrene miniemulsion polymerization (run 1 of Table 1) using the transfer agent 1 are shown as a function of conversion. It is seen that a good control of the polymerization was achieved, as indicated by the linear growth of  $M_n$  with conversion and by the low polydispersity values. This should in fact be compared with the cumulated polydispersity value in a batch reactor for a segregated system where bimolecular termination by combination is dominant. Since the corresponding instantaneous polydispersity is 2, larger values for the cumulated polydispersity are certainly obtained. However, the potential of this living mechanism is to produce more uniform MWDs, since smaller values have been obtained using bulk RAFT polymerization, usually ranging from 1.1 to 1.3.<sup>22</sup>

There are two types of possible explanations for the relatively large  $P_d$  values obtained in miniemulsion as compared to those that can be obtained in a bulk process. The first one relates to some imperfections in the behavior of the miniemulsion. Ideally, in fact, a miniemulsion should have particles all of the same size that are nucleated by radical entry all at the same time. Actually, the particles that are nucleated first (which clearly include preferentially the smaller particles) deplete faster the monomer, which is then replaced by the one coming from particles nucleated later. This leads to different RAFT agent concentrations in the different particles, thus causing differences in the average molecular weight produced in each particle and then a broadening of the MWD. This is actually the same concept described in the previous section under the

**Figure 4.** Experimental MWD curves at various conversion values for a styrene miniemulsion LRP with RAFT agent 1 (run 1 in Table 1). The arrow indicates the presence of a shoulder in the MWD.

second requirement, which we see then violated also in miniemulsion although to a much smaller extent than in the case of *ab initio* polymerization.

A second explanation deals with the adopted preparation of the RAFT agent 1 in Table 2. This was actually produced by bulk oligomerization starting from the RAFT agent 2, where the production of a small fraction of dead chains, i.e., which cannot restart propagating, is unavoidable. These short dead chains are probably responsible for the small peak in the low molecular weight tail of the normalized MWD (indicated by an arrow in the figure) obtained in the experimental run 1 and shown in Figure 4, which indeed caused a significant increase of  $P_d$ . On the other hand, the distributions shown in Figure 4 further support the living nature of the polymerization, as evidenced by the shift of the MWD peak toward larger molecular weights. The presence of dead chains in the RAFT agent 1 affects also the value of  $M_n = 37\,860$  g/mol, which is slightly larger than the theoretical one, calculated as the molar ratio between reacted monomer and dormant species at the same conversion (i.e.,  $M_n^h = (M_0/D_0)\chi = 34\,200$  g/mol, using the data in Table 1). This is in agreement with the observation that not all the chains in the RAFT agent were actually active; i.e., they could restart.

Summarizing, even if the reaction was clearly living and with a low number of terminations, slightly larger  $P_d$  values than in the corresponding bulk polymerization have been obtained. Two possible causes have been identified: one due to the presence in the RAFT agent of a fraction of dead chains unable to restart and one due to the possibility of having particles with different concentration of the RAFT agent.

Let us now consider the polymerization rate. It was found that 70% conversion was reached after 2 h of reaction (Table 1), which is slower than the equivalent nonliving miniemulsion polymerization. This can be seen by estimating the polymerization time for a styrene miniemulsion polymerization, assuming the average number of radicals per particle  $\bar{n} = 0.5$ , as typical for a 0–1 system.<sup>2</sup> If the miniemulsion droplets are supposed to behave as small batch reactors with constant volume, the following expression for the mass balance of the monomer is obtained:

$$\frac{dM}{dt} = -k_p MR \quad (5)$$



$M$  being the monomer concentration,  $R^*$  the radical concentration in the droplet ( $R^* = 0.5/N_A V_p$ , where  $N_A$  is Avogadro's constant and  $V_p$  the particle volume), and  $k_p$  the propagation rate constant. By integrating eq 5, the following expression for the polymerization time is obtained:

$$t = \frac{N_A V_p}{0.5 k_p} \ln\left(\frac{1}{1 - \chi}\right) \quad (6)$$

where  $\chi$  represents monomer conversion. Introducing the literature value  $k_p = 660 \text{ L}/(\text{mol s})^{32}$  and the experimental values  $V_p = 1.23 \times 10^{-18} \text{ L}$  (corresponding to a particle diameter of 133 nm) and  $\chi = 0.67$ , the estimated polymerization time is 0.7 h. This is in good agreement with the data by Blythe et al.,<sup>33,34</sup> who reported experimental polymerization times for styrene miniemulsion of about 1 h in similar conditions. On the other hand, this is shorter than the experimental value of 1.9 h measured in run 1, thus indicating that some delaying mechanism is present. Moad et al.<sup>22</sup> reported that a slow utilization of the RAFT agent may produce this "retardation effect". However, such a mechanism leads also to a clear initial induction period, which was instead not observed experimentally in this case. Most likely this polymerization rate decrease can be attributed to radical desorption from the polymer particles, as recently proposed by Monteiro et al.<sup>24</sup> for a seeded system. In particular, when the transfer agent RX undergoes the first exchange reaction, it produces a relatively short radical  $R^*$ , which may have some water affinity and therefore desorbs from the polymer particles. For example, the RAFT agent **1** is actually constituted by a mixture of species with different R groups which contain on average 12–13 styrene groups (corresponding to  $M_n = 1470 \text{ g/mol}$ ). The fraction of these containing zero or one groups is therefore not negligible, and these can lead to desorption from the polymer particles. This argument is supported by the kinetic behavior of runs 2 and 3 (see Table 1), initiated by the RAFT agent **2**. In this case, a much larger decrease of the polymerization rate was observed, in agreement with the fact that  $R^*$  is a *tert*-butyl radical ( $-\text{C}(\text{CH}_3)_3$ ) which has indeed a larger particle desorption probability. On the other hand, when RAFT agent **3**, which contains a long polystyrene chain, was used (see run 4), the reaction rate increased to values close to that typical of a nonliving miniemulsion polymerization with  $\bar{n}$  equal to 0.5.

Let us now examine the polymerization performance when using the RAFT agent **4**, which leads to reaction rates only slightly smaller than a conventional nonliving emulsion polymerization (cf. runs 5 and 6 in Table 1). This is consistent with the explanation given above, being the diffusivity of the styrene radical smaller than that of the *tert*-butyl radical. It is however surprising that the retardation effect due to the desorption of the RAFT agent **4** is much less pronounced than with the more bulky RAFT agent **1**. This could be explained by the presence of residual *tert*-butyl groups in the RAFT agent **1** which could then desorb faster than the styrene groups of RAFT agent **4**. However, additional work is needed to better elucidate this aspect.

From the linear increase of  $M_n$  with conversion shown in Figure 5 and from the shift of the MWD peak as a function of conversion shown in Figure 6, we can conclude that this is indeed a LRP. However, in Figure

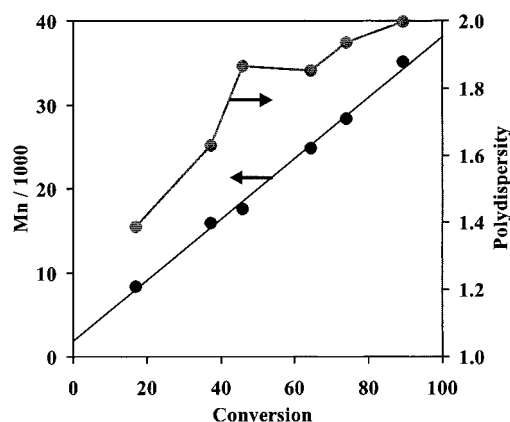


**Figure 5.** Experimental values of the number-average molecular weight,  $M_n$  (g/mol), and the polydispersity as a function of conversion for a styrene miniemulsion LRP with RAFT agent **4** (run 5 in Table 1).

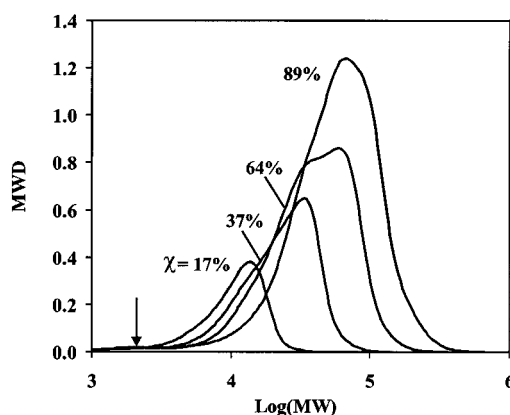


**Figure 6.** Experimental MWD curves at various conversion values for a styrene miniemulsion LRP with RAFT agent **4** (run 5 in Table 1). The arrow indicates the presence of a shoulder in the MWD.

5 it is also seen that relatively large values of  $P_d$  are obtained. It is difficult to explain the origin of these values, which are certainly connected both to a small peak in the low MW tail of the distribution (indicated by an arrow in Figure 6) as well as to the broadening of the MWD. This could be due to a loss of homogenization ability of the living mechanism, probably due again to a nonhomogeneous partitioning of the RAFT agent among the particles.

Thus, summarizing, slower kinetics have been generally found in styrene miniemulsion LRP than in the corresponding nonliving systems. This is probably due to the desorption of the radical formed by the first exchange reaction of the RAFT agent in the polymer particles. In particular, slow polymerization rates are associated with fast diffusing groups, while for highly water-insoluble groups (less prone to desorption) nonliving polymerization rates are obtained. On the other hand, it has been found that the broader MWDs are obtained when using RAFT agents containing water-insoluble groups, probably because of nonhomogeneous distribution of the active species (monomer and RAFT agent) among the particles.

These same conclusions have been drawn in the case of MMA LRP in miniemulsion. The polymerization of MMA has been performed in runs 7 and 9 until complete monomer conversion, using two RAFT agents with different but large molecular weight. Styrene has been added to the reactor after MMA was fully depleted in

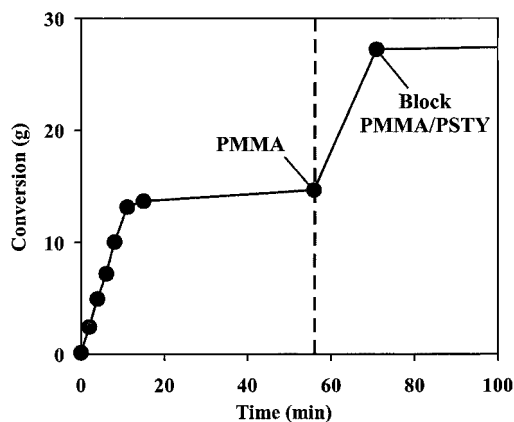


**Figure 7.** Experimental values of conversion as a function of reaction time for a methyl methacrylate-styrene miniemulsion block copolymerization with RAFT agent 5 (runs 7 and 8 in Table 1). Experimental points on the left of the dashed line refer to the methyl methacrylate homopolymerization (first block).

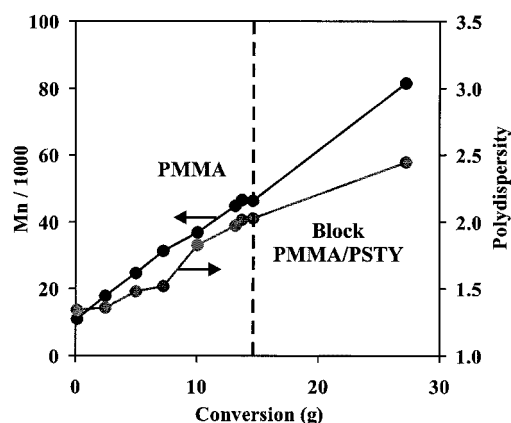


**Figure 8.** Experimental values of the number-average molecular weight,  $M_n$  (g/mol), and the polydispersity as a function of conversion for a methyl methacrylate-styrene miniemulsion block copolymerization with RAFT agent 5 (runs 7 and 8 in Table 1). Experimental points on the left of the dashed line refer to the methyl methacrylate homopolymerization (first block).

order to produce a block copolymer in runs 8 and 10 in Table 1. Although the fact that a block copolymer has been obtained is itself a proof of the living nature of the process, let us leave runs 8 and 10 aside for the moment and consider only the homopolymerization runs 7 and 9. From the data in Table 1 and Figure 7, it is seen that rather large polymerization rates are obtained in both cases. These are not only due to the large reactivity of MMA ( $k_p = 940 \text{ L}/(\text{mol s})$  at  $65^\circ\text{C}$ <sup>35</sup>) with respect to styrene ( $k_p = 660 \text{ L}/(\text{mol s})$  at  $80^\circ\text{C}$ <sup>32</sup>) but also to the very small droplet size obtained when preparing the miniemulsion with MMA (between 50 and 70 nm). In particular, when estimating the theoretical polymerization time by eq 6, a value close to the experimental one (9 min instead of 15 min) is obtained, which is again consistent with the high molecular weight RAFT agent used, which is unlikely to desorb. The corresponding  $P_d$  values, shown in the first part of Figure 8, are relatively large and grow in time. However, the linear increase of  $M_n$  and the shift of the MWD as a function of conversion shown in Figure 9 clearly prove the living nature of the polymerization.

The relatively poor result in terms of polydispersity can be again ascribed to a nonuniform concentration of

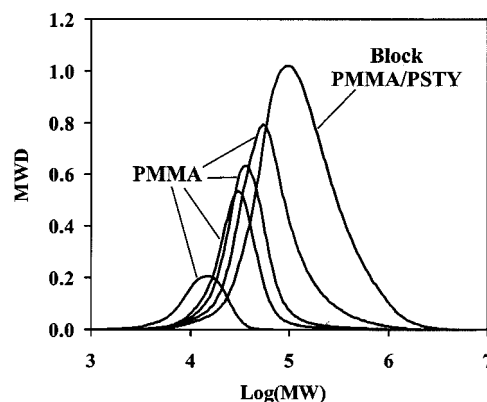


**Figure 9.** Experimental MWD curves at different conversion values for a methyl methacrylate-styrene miniemulsion block copolymerization with RAFT agent 5 (runs 7 and 8 of Table 1).

the dormant chains, due to the different reactivity of the different particles already mentioned in the case of styrene. Moreover, it is worth noting that, due to (i) the small frequency of decomposition of the initiator at the operating temperature, (ii) the large number of particles in the system, and (iii) the short duration of the polymerization, the particles generally experience few entries, whose average value can be estimated as equal to about 6. This means that a particle spends a remarkable part of the polymerization without radicals, thus acting only as a monomer reservoir for the reacting particles, which increases the difference in the dormant chain concentration among the particles. In run 9, the amount of initiator has been largely increased with respect to run 7, so that the particles can experience a larger number of entries (estimated as equal to about 15). However, only a slight improvement in terms of  $P_d$  was observed. Note that a further contribution to the relatively large polydispersities observed in this case could be due to homogeneous nucleation, as also observed by de Brouwers et al.<sup>25</sup> This could also explain the large tail observed in the MWD at large MWs (cf. Figure 9), typical of MMA growth under noncontrolled reaction conditions. However, no further evidences have been found to support this statement, and the particle size distribution as measured by light scattering was found to be monomodal.

Summarizing, even though a conclusive picture of all factors affecting the final performance of a RAFT polymerization in miniemulsion is not possible, some useful final conclusions can be drawn. First, the nature of the leaving group is affecting the polymerization rate, since small leaving groups can easily diffuse out of the particle. Second, even though the  $P_d$  values listed in Table 1 seem to indicate a better performance of RAFT agents with phenyl groups, we believe that no general conclusions can be drawn with this respect. In fact, similar results for bulk polymerization<sup>22,31</sup> do not indicate any significant difference between phenyl- and pyrrole-based RAFT agents. Moreover, the results in Table 1 indicate a strong correlation between polymerization rate and final  $P_d$  value. This could mean that process conditions more than the type of RAFT agent used are responsible for determining the final polydispersity.

Finally, the potential of living miniemulsion in producing block copolymers has been tested in runs 8 and 10, where styrene was added to the PMMA produced in runs 7 and 9, respectively. Because of the limited



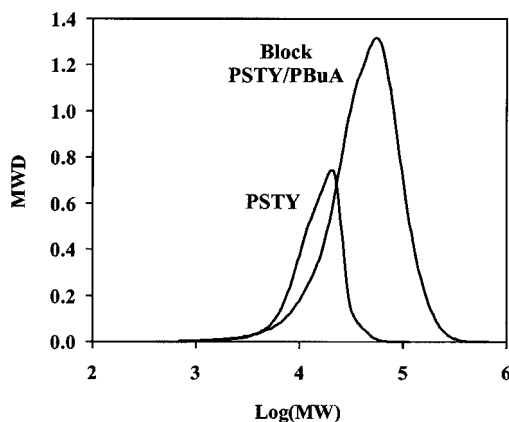


**Figure 10.** Experimental MWD curves just before the addition of the second monomer and at final conversion for a styrene–butyl acrylate miniemulsion block copolymerization with RAFT agent **4** (runs 11 and 12 in Table 1).

particle size, styrene completely reacted in less than 20 min, as indicated by the conversion values shown in Figure 7. Although the  $P_d$  values of the resulting block copolymers reported in Figure 8 are relatively large, the further shift of the MWD peak after the second reaction step (Figure 9) is a clear indication that the PMMA chains restarted, thus producing a block copolymer. This is also confirmed by the satisfying matching between the experimental  $M_n = 81\,450$  g/mol in run 8 and the corresponding  $M_n$  calculated using the data in Table 1, i.e.,  $M_n = M_{0\%}/D_0 = 79\,100$  g/mol.

The production of a different block copolymer of styrene and butyl acrylate was also performed (runs 11 and 12 in Table 2). It is worth noting that the second monomer (butyl acrylate) was added when the conversion of styrene was not complete and equal to about 63%. This could represent an interesting operating option to overcome the problem related to the different reactivities of the two monomers. Since the mutual propagation rates are well below the unity, a tapered structure of the copolymer is expected, as reported by Farcet et al.<sup>19</sup> By inspection of Figure 10, where the MWD of the styrene block before the addition of the second monomer and the MWD of the final block copolymer are shown, it is clear that the polymerization was proceeded by a living mechanism. Moreover, it is worth mentioning that neither the large polymer MWs typical of butyl acrylate polymerization nor gel formation was observed.

## 6. Conclusions

A comprehensive analysis combining modeling and experiments has been carried out to identify the best approach to the production of living polymers in heterogeneous system, so as to achieve controlled polymer microstructure with productivities much larger than in the corresponding living bulk process. The two key results are the identification of the most convenient living mechanism and the realization of a suitable process.

It has been shown that the RAFT (or DT) living mechanism is the optimal one since, due to the particular stoichiometry of the exchange reaction which does not affect the active chain concentration, it allows to achieve reaction rates comparable to those of the corresponding nonliving processes. The reason for this is that terminations are intrinsically reduced by segregation, as is typical for emulsion nonliving processes, and

larger values of the overall concentration of active species can be obtained without affecting the quality of the final product. The opposite conclusion has been reached when dealing with NLP and ATRP. In this case, the living mechanism forces the system to operate at small average number of radicals per particle and, thus, with small polymerization rates.

About the best way to segregate the system, problems related to the diffusion of the RAFT agent from the monomer droplets to the polymer particles arise when dealing with *ab initio* emulsion polymerization. Even though a partial solution can be found by properly tuning the diffusivity of the RAFT agent and the duration of the nucleation period, these difficulties are more simply prevented by using miniemulsion polymerization. In this case, the RAFT agent is already segregated in the reaction locus, and therefore more degrees of freedom are available to properly select the best RAFT agent for the specific application under examination.

To prove the reliability of these conclusions, experimental results have been reported for RAFT polymerization of different monomers in miniemulsion. The expected enhancement of the polymerization rate was actually observed, in particular when dealing with small polymer particles, as in the case of MMA. Moreover, the ability of controlling the polymer growth, particularly evident when low polydispersity values were obtained, and the possibility of producing block copolymers have been demonstrated. However, some important limitations have been identified, mainly related to the interparticle transport of the involved species. The droplet stabilization given by the hydrophobe is in fact not sufficient to prevent monomer diffusion from more reactive to less reactive particles in order to keep equilibrium conditions. This redistribution plays a negative role, since it affects the initial homogeneity of the RAFT agent concentration in the polymer particles. With this respect, RAFT agents with high mobility should minimize these problems. However, it has been verified experimentally that RAFT agents with too large water solubility reduce the polymerization rate, as a consequence of the larger desorption rate.

In conclusion, it has been shown that the RAFT mechanism in miniemulsion polymerization can provide living polymerization at reaction rates comparable to the corresponding nonliving processes. This result makes it possible to produce at the industrial scale well controlled polymers as well as block copolymers by free radical polymerization. Further improvements on the polydispersity values can be obtained by improving the interphase partitioning of the involved species.

## Appendix: Diffusion Model for RAFT Agent in *ab Initio* Emulsion Polymerization

The development of a very simplified model of *ab initio* emulsion polymerization accounting for diffusion limitations of the RAFT agent from the monomer droplets to the particles and particle nucleation is reported. First, let us summarize the main assumptions underlying the model equations.

**Constant Nucleation Rate.** For example, this situation could be actually approached at the beginning of the reaction, when the surface of the micelles is largely dominant with respect to the surface of droplets and particles, so that most of the radicals produced by the initiator at a constant rate are entering them. Even

though this is never the case because of variations of the initiator concentration, aqueous phase terminations, and competition for radical entry, this assumption is simplifying the model equations without affecting the conclusions of the theoretical analysis. As a consequence, the particle number ( $N_p$ ) is readily evaluated as proportional to time:

$$N_p = K_1 t \quad (7)$$

and the duration of the nucleation period,  $t_N$ , is set by fixing the final number of particles,  $N_p^f$ .

**Constant Particle Volume Growth Rate.** This corresponds to the typical case of an emulsion with constant number of active chains per particle during the first two intervals of the reaction (i.e., in the presence of monomer droplets). The corresponding equation for the overall volume of the particles is

$$\frac{dV_p}{dt} = k_p \bar{n} \frac{\phi_m}{1 - \phi_m} \frac{N_p}{N_A} = K_2 N_p \quad (8)$$

where  $k_p$  indicates the propagation rate constant,  $\bar{n}$  the average number of radicals per particle ( $\approx 0.5$ ), and  $\phi_m$  the monomer volume fraction inside the particle. Because of the very limited amount of RAFT agent used, this corresponds to the saturation value for the pure monomer and, in the presence of monomer droplets, is constant. If the expression for  $N_p$  from eq 7 is used in eq 8 and the time integration is carried out, the following expression is found:

$$V_p = \frac{K_1 K_2}{2} t^2 = \frac{K_2}{2 K_1} N_p^2 \quad (9)$$

Indicating as  $V_p^{\text{nuc}}$  the value of the overall particle volume at which the number of particles becomes equal to the final value  $N_p^f$ , the proportionality constant in eq 9 can be expressed as  $V_p^{\text{nuc}}/(N_p^f)^2$ . Therefore, the relationship between particle volume and number becomes

$$N_p = \frac{1}{N_p^f} \left( \frac{V_p}{V_p^{\text{nuc}}} \right)^2 \quad (10)$$

If the density of the monomer is assumed equal to that of the polymer, the polymerization takes place at constant volume of organic phases, and the final volume of a single particle is estimated as  $V_p^f = V_m^0/N_p^f$ , where  $V_m^0$  is the initial overall volume of monomer. Using eq 10 for  $N_p$ , the final version of the equation used to evaluate the particle number is

$$N_p = \begin{cases} (V_m^0/V_p^f)(V_p/V_p^{\text{nuc}})^{1/2} & \text{for } V_p \leq V_p^{\text{nuc}} \\ (V_m^0/V_p^f) & \text{for } V_p > V_p^{\text{nuc}} \end{cases} \quad (11)$$

**Diffusion Limitation for the RAFT Agent.** The last main assumption concerns the material transport of the RAFT species from the droplets to the particles through the aqueous phase. According to the literature (cf. Nomura et al.<sup>36</sup>), the rate-determining step is the diffusion out of the droplets. If in addition we assume (i) the RAFT agent with infinite reactivity and (ii) constant droplet size,  $v_D$ , determined by the operating conditions,<sup>36</sup> the following expression is used to evaluate the overall volume of RAFT agent inside the droplets:

$$\frac{dV_{D,ra}}{dt} = -2\pi D_{ra} r_D N_D \alpha_{ra} = -K_4 N_D \alpha_{ra} \quad (12)$$

where  $N_D$  indicates the total (variable) number of droplets and  $\alpha_{ra}$  the volume fraction of the RAFT agent in the droplet phase. By neglecting the monomer solubility in aqueous phase,  $N_D$  is readily evaluated as  $(V_m^0 - V_p)/v_D$ , where, as before, the amount of RAFT agent is neglected when calculating the volume of the phase. If  $\alpha_{ra}$  is expressed in terms of the ratio  $V_{D,ra}/(V_m^0 - V_p)$ , the following expression is obtained:

$$\frac{dV_{D,ra}}{dV_p} = -\frac{K_4}{K_2} \frac{V_{D,ra}}{v_D N_p} \quad (13)$$

Making the ratio between this equation and eq 8, the following balance is found:

$$\frac{dV_{D,ra}}{dt} = \begin{cases} -(\sigma/\eta)(\gamma/\chi)^{1/2} V_{D,ra} & \text{for } \chi \leq \gamma \\ -(\sigma/\eta) V_{D,ra} & \text{for } \chi > \gamma \end{cases} \quad (14)$$

In terms of conversion,  $\chi = V_p/V_m^0$ , this equation becomes

$$\frac{dV_{D,ra}}{d\chi} = \begin{cases} -(\sigma/\eta)(\gamma/\chi)^{1/2} V_{D,ra} & \text{for } \chi \leq \gamma \\ -(\sigma/\eta) V_{D,ra} & \text{for } \chi > \gamma \end{cases} \quad (15)$$

where the following adimensional groups have been introduced:  $\sigma = K_4/K_2$ ,  $\eta = v_D/v_p^f$  and  $\gamma = V_p^{\text{nuc}}/V_m^0$ . This differential equation is solved analytically to give

$$\frac{V_{D,ra}}{V_{D,ra}^0} = \begin{cases} \exp[-2(\sigma/\eta)(\gamma\chi)^{1/2}] & \text{for } \chi \leq \gamma \\ \exp[-(\sigma/\eta)(\gamma + \chi)] & \text{for } \chi > \gamma \end{cases} \quad (16)$$

Accordingly, the volumetric fraction of the RAFT agent in the droplets can be considered a function of its initial overall volume  $V_{D,ra}^0$ , of the monomer conversion,  $\chi$ , of the "length" of nucleation,  $\gamma$ , and of the parameter  $\sigma/\eta$ , related to the rate of diffusion.

The amount of RAFT agent,  $Q$ , which entered a particle nucleated at time  $t_B$  up to the end of the reaction,  $t_R$ , is now evaluated as

$$Q = \int_{t_B}^{t_R} \frac{K_4 N_D \alpha_{ra}}{N_p} dt \quad (17)$$

and, after algebraic manipulations, the following normalized quantity  $Q^*$  is obtained:

$$Q^* = Q \left( \frac{\sigma}{\eta} \frac{V_p^f}{V_m^0} \frac{V_{D,ra}^0}{V_{D,ra}^0} \right) = \gamma \int_{\gamma_B}^{\gamma} \frac{1}{\chi} \exp\left(-2\frac{\sigma}{\eta}\sqrt{\gamma\chi}\right) d\chi + \int_{\gamma}^1 \exp\left(-\frac{\sigma}{\eta}(\gamma + \chi)\right) d\chi \quad (18)$$

The integrals in eq 18 can be evaluated analytically, and the following final expression of  $Q^*$  is obtained, where the incomplete gamma function  $\Gamma$  is involved:

$$Q^* = 2\gamma \left[ \Gamma\left(0.2\frac{\sigma}{\eta}\sqrt{\gamma\chi_B}\right) - \Gamma\left(0.2\frac{\sigma}{\eta}\gamma\right) \right] + \frac{\sigma}{\eta} \left[ \exp\left(-2\frac{\sigma}{\eta}\gamma\right) - \exp\left(-\frac{\sigma}{\eta}(1 + \gamma)\right) \right] \quad (19)$$

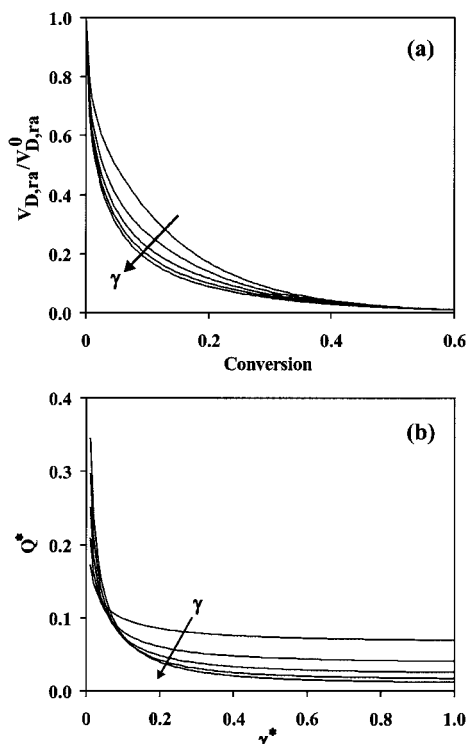


**Figure 11.** (a) Normalized overall volume of RAFT agent inside the droplets as a function of conversion evaluated for various nucleation lengths ( $\gamma = 0.05, 0.1, 0.15, 0.2$ , and  $0.25$ ). (b) Distribution of the RAFT agent among the particles as a function of the normalized period of nucleation  $\gamma^* = \gamma/\chi$  ( $\gamma = 0.05, 0.1, 0.15, 0.2$ , and  $0.25$ ).

Notably, according to eq 19,  $Q^*$  is a function of birth conversion  $\chi_B$  and of the two quantities  $\sigma/\eta$  and  $\gamma$ .

Using this equation, a series of parametric calculations have been carried out, aimed to compute the distribution  $Q^*$  of the overall amount of dormant species entered a particle as a function of its "age". Note that the duration of the nucleation period  $\gamma$  has been normalized in the following as  $\gamma^* = \gamma/\chi$  so that nucleation always stops for  $\gamma^* = 1$ .

As reported in section "Choice of the Living Mechanism", two basic requirements must be fulfilled in order to establish living conditions in an ab initio emulsion polymerization: (i) diffusion of the RAFT agent to the polymer particles in a time short compared to the entire duration of the process and (ii) homogeneous distribution of the RAFT agent among the particles. To fulfill the first requirement, we ask that 99% RAFT agent diffuse to the particle before 60% conversion. According to eq 16, this results in a specific relationship between the values of  $\gamma$  and  $\sigma/\eta$ , i.e.,  $\sigma/\eta = 4.605/(\gamma + 0.6)$ . This constraint has been fulfilled in all simulations reported in Figure 11a, where the evolution with conversion of the ratio between the volume of RAFT agent in the droplets and the initial value,  $V_{D,ra}/V_{D,ra}^0$ , is shown at different values of the length of the nucleation,  $\gamma$ . Note that for shorter nucleation periods the final number of particles is achieved earlier, and thus, the overall polymerization rate becomes faster with respect to the rate of diffusion. This effect of the nucleation duration is anyhow much less important than that on the distribution of the RAFT agent among the particles,  $Q^*$ , shown in Figure 11b. It can be seen that the longer the nucleation duration, the larger the difference in the amount of RAFT agent among the first and the last

nucleated particles. In fact, when the nucleation is fast, a large fraction of the RAFT agent diffuses to the particles only after the end of nucleation, when all the particles are already formed, thus resulting in a more homogeneous distribution of the RAFT agent availability.

Note that the previous discussion was focused on the overall amount of RAFT agent in the particle,  $Q^*$ . Since particles nucleated earlier grow more than those nucleated later, they have a larger volume and therefore the differences in concentration of RAFT agent are smaller than those in terms of the overall amount,  $Q^*$ . However, this compensation is very small, and similar differences remain also for the concentration values, which actually control the kinetics of the process. This can be seen by considering for example the case with the longer nucleation period (i.e.,  $\gamma = 0.25$ ), where this counterbalancing effect should be maximum. Under the assumptions given at the beginning of this Appendix, it can be shown that the volume added by a particle created at the beginning of the process ( $V_p = 0$ ) during the nucleation period is equal to  $2V_p^f\gamma$ , while the volume added by each particle after the end of the nucleation is  $V_p^f(1 - \gamma)$ . Accordingly, the ratio of the volumes of two particles nucleated at the beginning and at the end of the nucleation period is given by  $(1 - \gamma)/(1 + \gamma) = 0.6$ . This correction factor is not sufficient for compensating the difference of about 1 order of magnitude in terms of the overall amount of RAFT agent present in the two particles, which has been discussed above.

Thus concluding, a suitable tuning between RAFT agent diffusivity and nucleation rate is essential to ensure a homogeneous distribution of the active component among the particles. Namely, the nucleation has to be fast with respect to the RAFT agent diffusion which, in turn, has to be fast also with respect to the reaction time. This finding is in agreement with the discussion reported in the main body of this work and, even though not impossible, is quite difficult to be achieved in practice.

## References and Notes

- (1) Moad, G.; Solomon, D. H. *The Chemistry of Free-Radical Polymerization*; Pergamon: Oxford, 1995.
- (2) Gilbert, R. G. In *Emulsion Polymerization. A Mechanistic Approach*; Ottewill, R. H., Rowell, R. L., Eds.; Academic Press: London, 1995.
- (3) Matyjaszewski, K. *Controlled Radical Polymerization*; ACS Symp. Ser. Vol. 685; American Chemical Society: Washington, DC, 1997.
- (4) Greszta, D.; Matyjaszewski, K. *Macromolecules* **1996**, *29*, 7661.
- (5) Matyjaszewski, K.; Patten, T. E.; Xia, J. *J. Am. Chem. Soc.* **1997**, *119*, 674.
- (6) Goto, A.; Ohno, K.; Fukuda, T. *Macromolecules* **1998**, *31*, 2809.
- (7) Chong, B. Y. K.; Le, T. P. T.; Moad, G.; Rizzardo, E.; Thang, S. H. *Macromolecules* **1999**, *32*, 2071.
- (8) Bon, S. A. F.; Bosveld, M.; Klumperman, B.; German, A. L. *Macromolecules* **1997**, *30*, 324.
- (9) Marestin, C.; Noel, C.; Guyot, A.; Claverie, J. *Macromolecules* **1998**, *31*, 4041.
- (10) Prodpran, T.; Dimonie, V. L.; Sudol, E. D.; El-Aasser, M. S. *Macromol. Symp.* **2000**, *155*, 1.
- (11) MacLeod, P. J.; Barber, R.; Odell, P. G.; Keoshkerian, B.; Georges, M. K. *Macromol. Symp.* **2000**, *155*, 31.
- (12) Farcet, C.; Lansalot, M.; Charleux, B.; Pirri, R.; Vairon, J. P. *Macromolecules* **2000**, *33*, 8559.
- (13) Gaynor, S. G.; Qiu, J.; Matyjaszewski, K. *Macromolecules* **1998**, *31*, 5951.
- (14) Qiu, J.; Gaynor, S. G.; Matyjaszewski, K. *Macromolecules* **1999**, *32*, 2872.



- (15) Qiu, J.; Pintauer, T.; Gaynor, S. G.; Matyjaszewski, K.; Charleux, B.; Pirri, R.; Vairon, J. P. *Macromolecules* **2000**, *33*, 7310.
- (16) Matyjaszewski, K.; Qiu, J.; Tsarevsky, N. V.; Charleux, B. *J. Polym. Sci., Part A: Polym. Chem.* **2000**, *38*, 4724.
- (17) Lansalot, M.; Farcet, C.; Charleux, B.; Vairon, J. P.; Pirri, R. *Macromolecules* **1999**, *32*, 2537.
- (18) Butté, A.; Storti, G.; Morbidelli, M. *Macromolecules* **2000**, *33*, 3485.
- (19) Farcet, C.; Lansalot, M.; Pirri, R.; Vairon, J. P.; Charleux, B. *Macromol. Rapid Commun.* **2000**, *21*, 921.
- (20) Uzulina, I.; Kanagasabapathy, J.; Claverie, J. *Macromol. Symp.* **2000**, *150*, 33.
- (21) Charmot, D.; Corpart, P.; Adam, H.; Zard, S. Z.; Biadatti, T.; Bouhadir, G. *Macromol. Symp.* **2000**, *150*, 23.
- (22) Moad, G.; Chiefari, J.; Chong, B. Y. K.; Krstina, J.; Mayadunne, R. T. A.; Postma, A.; Rizzardo, E.; Thang, S. H. *Polym. Int.* **2000**, *49*, 993.
- (23) Monteiro, M. J.; Sjöberg, M.; van der Vlist, J.; Gottgens, C. M. *J. Polym. Sci., Part A: Polym. Chem.* **2000**, *38*, 4206.
- (24) Monteiro, M. J.; Hodgson, M.; De Brouwer, H. *J. Polym. Sci., Part A: Polym. Chem.* **2000**, *38*, 3864.
- (25) De Brouwer, H.; Tsavalas, J. G.; Schork, F. J.; Monteiro, M. *J. Macromolecules* **2000**, *33*, 9239.
- (26) Butté, A.; Storti, G.; Morbidelli, M. *Chem. Eng. Sci.* **1999**, *54*, 3225.
- (27) Fischer, H. *Macromolecules* **1997**, *30*, 5666.
- (28) Charleux, B. *Macromolecules* **2000**, *33*, 5358.
- (29) Butté, A.; Storti, G.; Morbidelli, M. *J. Polym. Sci., Part A: Polym. Chem.*, submitted.
- (30) Gaynor, S. G.; Wang, J. S.; Matyjaszewski, K. *Macromolecules* **1995**, *28*, 8051.
- (31) Mayadunne, R. T. A.; Rizzardo, E.; Chiefari, J.; Chong, B. Y. K.; Moad, G.; Thang, S. H. *Macromolecules* **1999**, *32*, 6977.
- (32) Buback, M.; Gilbert, R. G.; Hutchinson, R. A.; Klumpermann, B.; Kuchta, F. D.; Manders, B. G.; O'Driscoll, K. F.; Russel, G. T.; Schweer, J. *Makromol. Chem. Phys.* **1995**, *196*, 3267.
- (33) Blythe, P. J.; Morrison, B. R.; Mathauer, K. A.; Sudol, E. D.; El-Aasser, M. S. *Langmuir* **2000**, *16*, 898.
- (34) Blythe, P. J.; Sudol, E. D.; El-Aasser, M. S. *Macromol. Symp.* **2000**, *150*, 179.
- (35) Beuermann, S.; Buback, M.; Davis, P. D.; Gilbert, R. G.; Hutchinson, R. A.; Olaj, O. F.; Russel, G. T.; Schweer, J.; van Herk, A. M. *Makromol. Chem. Phys.* **1997**, *198*, 1545.
- (36) Nomura, M.; Suzuki, H.; Tokunaga, H.; Fujita, K. *J. Appl. Polym. Sci.* **1994**, *51*, 21.

MA002130Y